iJRASET
International Journal For Research in Applied Science and Engineering Technology

INTERNATIONAL JOURNAL FOR RESEARCH

IN APPLIED SCIENCE & ENGINEERING TECHNOLOGY

Volume: 6 **Issue:** XI **Month of publication:** November 2018

DOI:

www.ijraset.com

Call: 08813907089 | E-mail ID: ijraset@gmail.com

International Journal for Research in Applied Science & Engineering Technology (IJRASET)
ISSN: 2321-9653; IC Value: 45.98; SJ Impact Factor: 6.887
Volume 6 Issue XI, Nov 2018- Available at www.ijraset.com

Effect of Lanthanum Doping on Bismuth Ferrite ($BiFeO_3$) for Solar Cell Applications

Sovia[1], Amit Kumar[2], Kulwinder Singh[3], Jaswinder Pal[4]
[1]*Research Scholar, Department of Electronics and Communication Engineering, MRS Punjab Technical University, Jalandhar, Punjab, India*
[2, 3, 4]*Department of Electronics and Communication Engineering, Bhai Maha Singh College of Engineering, Sri Muktsar Sahib, Punjab, India*

Abstract: ***Single phase $Bi_{1-x}La_xFeO_3$ $(0.1\leq x\leq 0.3)$ ceramics have been successfully synthesized using conventional solid state reaction route. The XRD analysis reveals that all the samples possess rhombohedral structure. The doping of La (Lanthanum) in $BiFeO_3$ at varying concentrations (x=0.1, 0.2 and 0.3) have been observed to decrease its band gap and make it optimum choice for solar cell application. La doping enhanced the magnetic properties of $BiFeO_3$ and also increases the Neel temperature and Dielectric Constant. EDAX confirms the absence of any other elemental properties except Bi, La, O, and Fe. The UV Visible spectrum for $Bi_{1-x}La_xFeO_3$ $(0.1\leq x\leq 0.3)$ ceramics concludes the decrease in band gap value. The sample x=0.2 exhibits a low value of ε' and a high value of ε'' in low frequency region implying the presence of high electric current in the sample. The ac conductivity data reveals that sample x=0.2 exhibits higher value of electrical conductivity. It has been observed that La doped Bismuth Ferrite at x=0.2 is suitable material for solar cell application.***

I. INTRODUCTION

Due to vast demand of electrical energy in this modern era, Solar Cell serves as the best source of renewable energy. It consumes electromagnetic waves from Sun and utilizes this energy into various technological applications. The main feature which differentiates a solar cell from another type of solar cell is the material of which it is made and the technology which is used up in designing a solar cell. The pervoskite $BiFeO_3$ being cheap, abundant and stable materials which can be used for solar cell application. It is a material which possesses ferro-electricity, ferro-magnetism and ferro-elasticity in a single phase [1, 2]. In present work, we report the synthesis of $Bi_{1-x}La_xFeO_3$ materials with composition ranging from x=0.1 to x=0.3 by using conventional solid state reaction route. The structural, magnetic, optical and dielectric properties of resulting materials have been discussed in detail.

II. EXPERIMENTAL DETAILS

Various samples of La doped $BiFeO_3$ (Bismuth Ferrite) prepared using conventional solid state reaction route. The raw materials Bi_2O_3, La_2O_3, Fe_2O_3 (99% purity) were taken in a stoichiometric proportions. Then these were ball milled for 24 hours using Zircona balls to obtain fine particle size and were placed in planetary ball mill for 6 hours. In order to facilitate the reaction of metal oxides, these are heated to higher temperature. The powders are then subjected to temperature (950^0C) for calcinations. It causes the constituents to react by inner diffusion of their ions and resulting in a homogeneous compound. After calcinations, PVA (poly vinyl alcohol) mixing is done. Then the pellets of 10 mm were formed using uni-axial hydraulic press at 10 tones pressure. The final stage of preparation of ceramics by solid state route ends with sintering which provides desertification (>95%). The XRD data of the sintered samples was obtained using D8 Focus X-Ray diffraction system (Cu Kα radiation of 1.5418 Å). Carl Zeiss Supra 55 scanning electron microscope was used to study the surface morphology. The magnetic properties were studied using Microsence E29 VSM. Dielectric measurements of the samples were carried out using computerized measurement set up. The UV-Vis spectrum was used to calculate the band gaps of semiconductor material by plotting the graph between $(\alpha h\upsilon)^{1/2}$ versus photon energy ($h\upsilon$).

III. RESULTS & DISCUSSION

The X-ray diffraction technique has been used to study the effect of La substitution on the structure of BFO. Figure 1 (a-c) shows XRD patterns for $Bi_{1-x}La_xFeO_3$ ceramics for x= 0.1, x=0.2, x= 0.3 in fig (a), (b), (c) respectively. It shows that the XRD pattern of all samples can be indexed according to the rhombohedral structure having space group *R3c*. No impurity phase has been detected. Lebail refinement of all samples has been carried out using FULLPROF software for detailed structural analysis [3]. The samples ranging from x= 0.0.1 to x= 0.3 possess a rhombohedral structure of R3C group as stated by Lebail refinement results. It can be seen from Fig. 1 that the sample x=0.3 shows the Doublet reflections at 2θ values ≈ 32˚, 39˚, 51˚ and 57˚. For x =0.3 sample, there seems

to be asymmetrical broadening of the peaks and this splitting of peaks is not visible to naked eye. Thus, the x=0.3 sample exhibits pseudo-cubic structure. This depicts low symmetry of a crystal structure. With increase in La concentration, there is a decrease in the fraction of rhombohedral phase. This phase transition from rhombohedral (space group *R3c*) to pseudo-cubic structure is due to the presence of of La^{3+} ions into the BFO lattice. This distortion is caused due to difference in ionic radii of Bi^{3+} (1.17 Å) and La^{3+} (1.24 Å) and also increases with increasing La concentration. The calculated values of lattice parameters, c/a ratio, goodness of fit (GOF) and cell volume are summarized in Table 1.

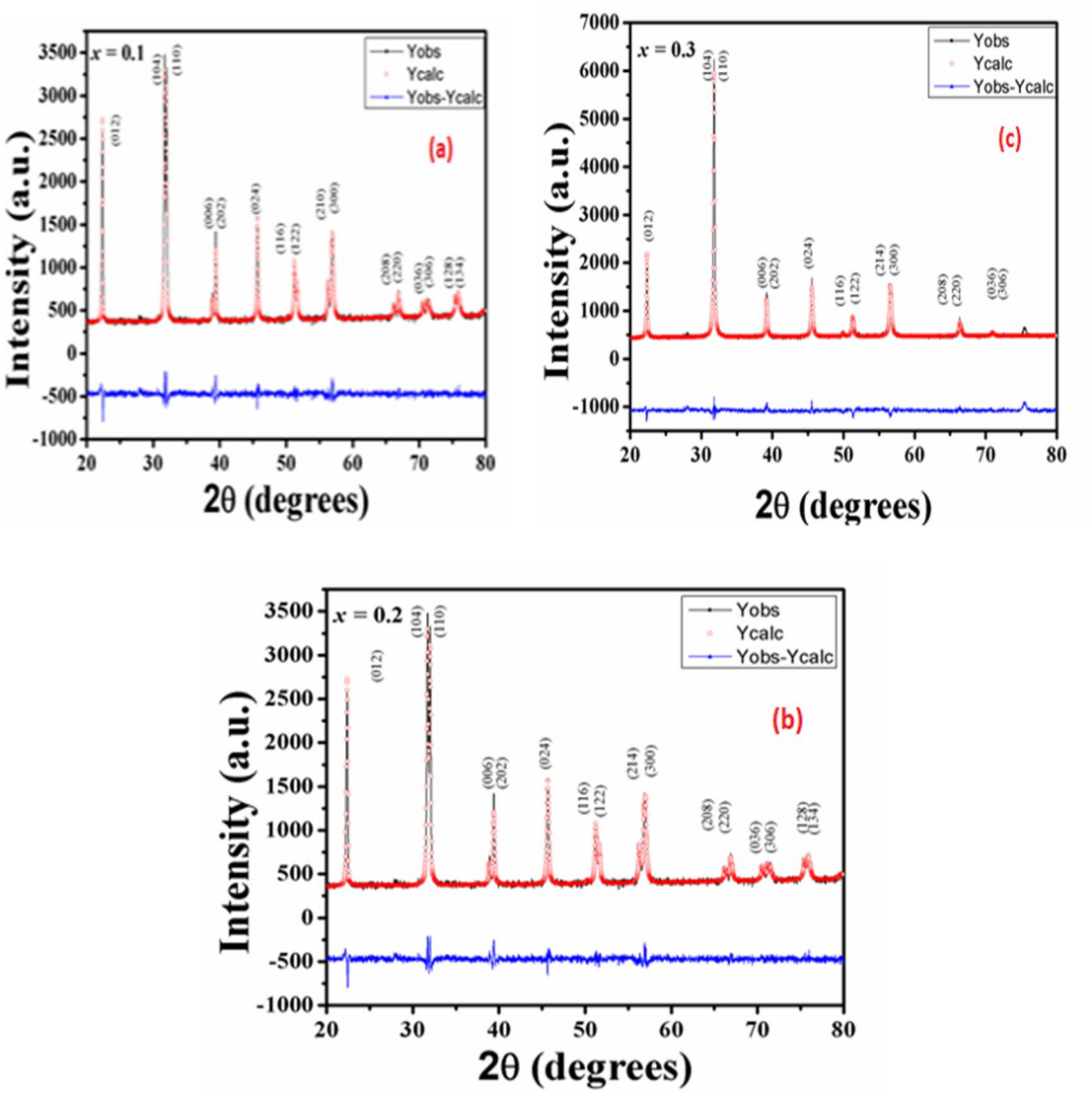

Fig. 1: Lebail calculated and difference plots of XRD for $Bi_{1-x}Gd_xFeO_3$ (x=0.1, 0.2, 0.3)

Table 1: Lebail refined parameters of $Bi_{1-x}La_xFeO_3$ samples for x=0.1, x=0.2, x= 0.3

Composition	a[Aº]	c[Aº]	c/a	gof	Chi^2	Volume[$(Aº)^3$]
x=0.1	3.922	4.122	1.05099	1.3	1.53	63.40
x=0.2	3.933	4.008	1.01906	1.7	1.57	61.99
x=0.3	3.991	3.999	1.00200	1.3	1.89	63.70

The sintered samples in the form of a pellet of the prepared material were taken for SEM. The SEM used was Carl Zeiss Supra55. Scanning electron graphs of all sintered samples are obtained at 20 KX magnifications. The SEM Micrographs are shown in figure 2.1 (a-c) for $Bi_{1-x}La_xFeO_3$ where x=0.1, x=0.2, x=0.3. The graphs clearly indicated the homogeneous, well interlinked, randomly oriented and no uniform nature of grains. The average grain size has been observed for x=0.1 is 3.25 µm (approximately), for x=0.2 is 7.05 µm (approximately), and for x=0.3 is 2.91 µm (approximately). The average grain size starts increasing from x=0.1 to x=0.2. With further increase in doping level (x=0.3) the grain size decreases. The largest average grain size and better grain homogeneity is obtained for sample *x*=0.2. Grain growth in these solid solutions is due to the substitution of La in $BiFeO_3$ system. It is reported in literature that the partial substitution of La at A-site helps in grain growth and densification of the solid solutions [4-5].

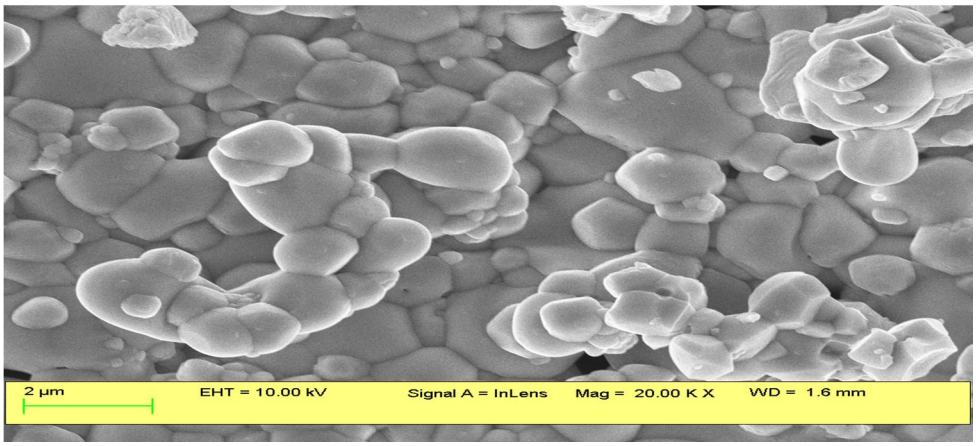

Fig. 2 (a) SEM Micrograph for $Bi_{1-x}La_xFeO_3$ (x=0.1) sample

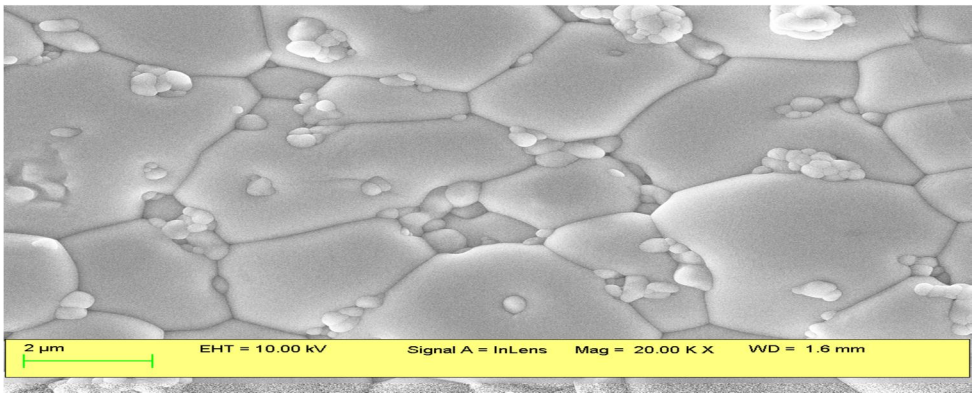

Fig. 2 (b) SEM Micrograph for $Bi_{1-x}La_xFeO_3$ (x=0.2) sample

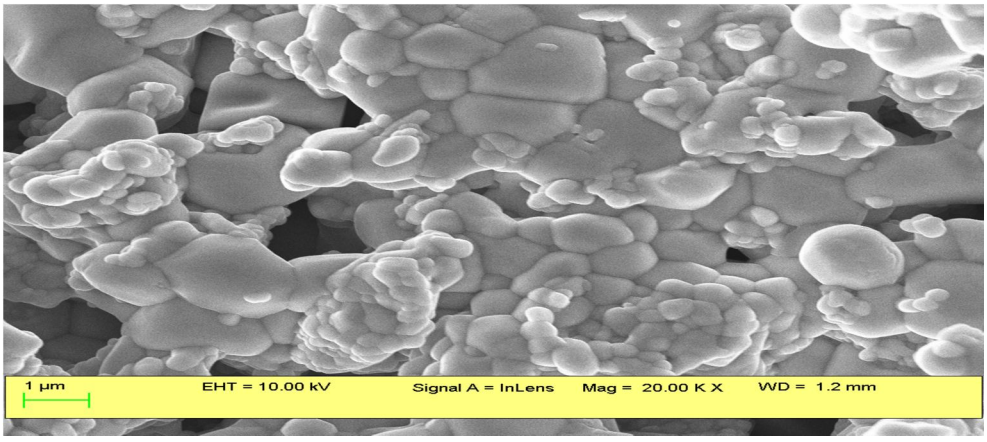

Fig. 2 (c) SEM Micrograph for $Bi_{1-x}La_xFeO_3$ (x=0.3) sample

ISSN: 2321-9653; IC Value: 45.98; SJ Impact Factor: 6.887
Volume 6 Issue XI, Nov 2018- Available at www.ijraset.com

EDAX Spectras for $Bi_{1-x}La_xFeO_3$ ($0.1 \leq x \leq 0.3$) are shown in figure 3 (a-c). It is clearly seen from EDAX spectra that the prepared ceramics contains only of Bi, La, Fe and O. There are no other elemental impurities. The actual stochiometric composition matches well with the elemental composition obtained from EDAX spectra.

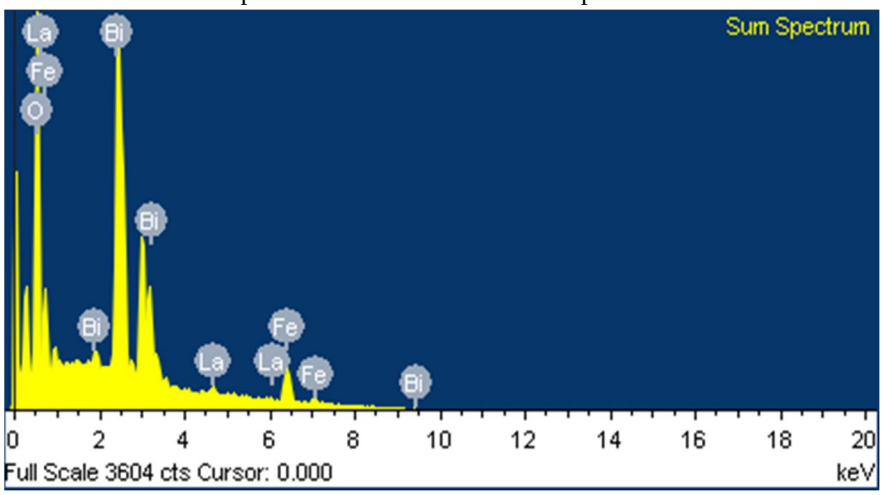

Element	Weight%
O K	20.77
Fe L	19.17
La L	3.48
Bi M	56.58
Totals	100.00

Fig. 3 (a): Energy Dispersive X-Ray analysis for $Bi_{1-x}La_xFeO_3$ (x=0.1) sample.

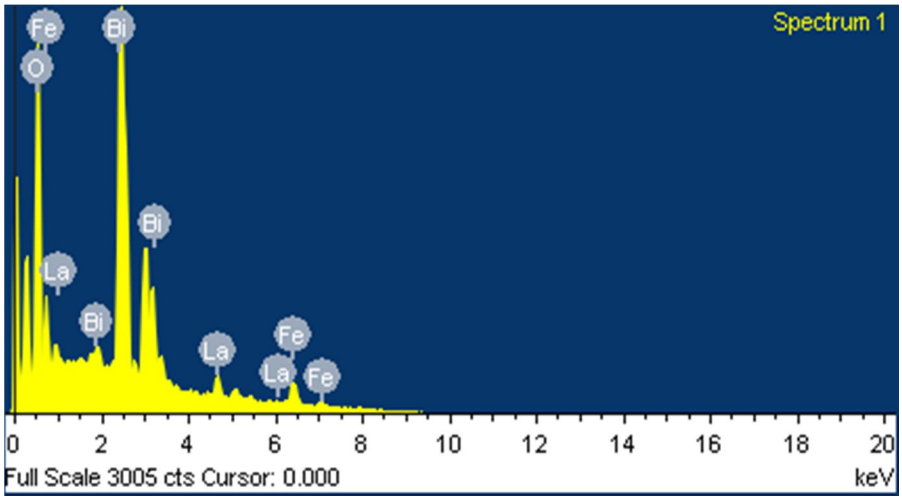

Element	Weight%
O K	18.65
Fe L	14.95
La L	10.48
Bi M	55.92
Totals	100.00

Fig. 3 (b): Energy Dispersive X-Ray analysis for $Bi_{1-x}La_xFeO_3$ (x=0.2) sample.

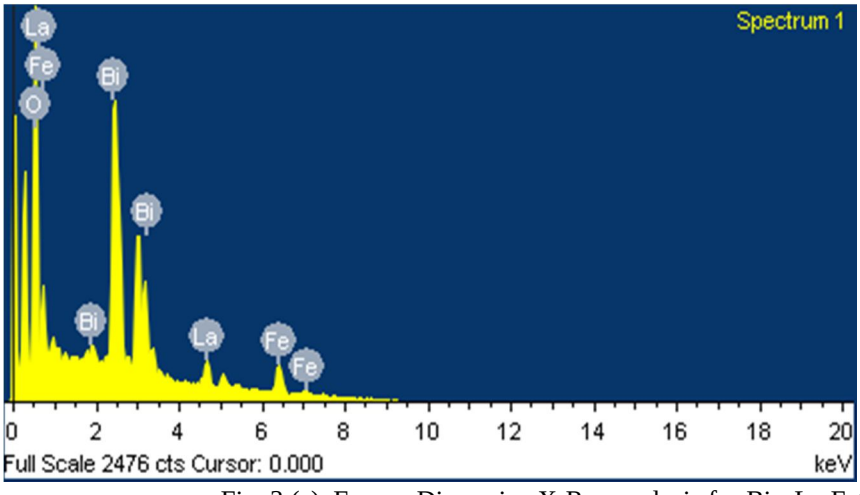

Element	Weight%
O K	19.67
Fe L	18.18
La L	16.34
Bi M	45.80
Totals	100.00

Fig. 3 (c): Energy Dispersive X-Ray analysis for $Bi_{1-x}La_xFeO_3$ (x =0.3) sample.

The UV visible spectrum for $Bi_{1-x}La_xFeO_3$ ($0.1 \leq x \leq 0.3$) samples is shown in Fig. 4. The wavelength used is 200nm to 900 nm. The Tauc's plots $((\alpha\hbar\omega)^{1/2}$ versus energy) are derived from absorption versus wavelength graphs. The calculated values of Bandgap from Tauc's plot are 2.01 eV, 1.72 eV and 2.46 eV for x=0.1, x=0.2 and x=0.3, respectively. Calculated value of band gap in case of pure $BiFeO_3$ (BF) is 2.11 eV [6]. It is clear that the band gap starts decreasing with doping from x= 0.1 to x=0.2. With further addition of x in BF (for x=0.3) the value of band gap increases as compared to pure BF. So it is concluded that the x=0.2 sample is the most suitable candidate for solar cell applications.

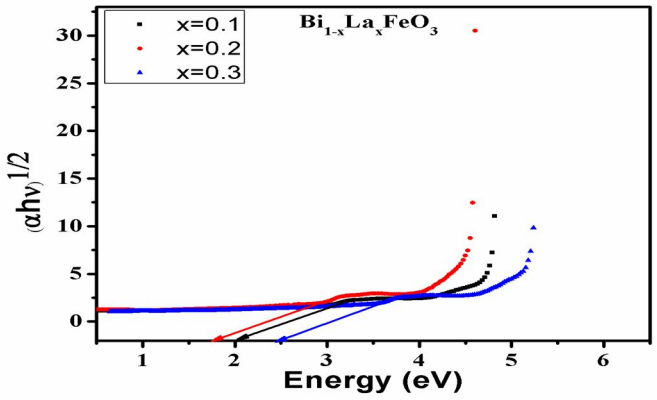

Fig. 4: The Tauc's plots $((\alpha\hbar\omega)^{1/2}$versus energy) for $Bi_{1-x}La_xFeO_3$ ($0.1 \leq x \leq 0.3$) ceramics.

Figures 5 (a) and (b) show the frequency dependence of dielectric constant and dielectric loss for $Bi_{1-x}La_xFeO_3$ (x= 0.1, 0.2 and 0.3) at room temperature. The operated frequency range is 100 Hz – 100 KHz. The figures clearly indicated the inverse relation of dielectric constant and dielectric loss with frequency. The rate of decrease of observed quantities is high in lower frequency range and small in high frequency range. Dipole relaxation formula explains the observed relations [7]. Various polarizations such as dipolar, ionic, electronic and interfacial polarizations sum up to the net polarization. At lower frequencies, time varying electric filed affects all these polarizations and increases the total polarization due to which higher values of dielectric constant and dielectric loss are obtained. But at higher frequencies, rate of varying electric field is quite high and dipole orientations cannot switch a fast as electric field resulting in small net polarization and smaller values of dielectric constant and dielectric loss. The Figures 5 (a) and (b) clear that sample at x=0.2 exhibit low value of dielectric constant and high value of dielectric loss in low frequency region. The high value of ε″ implies the presence of high electric current in the sample. The possible reason can be the narrow band gap of the sample. So is concluded that the x=0.2 sample is the most suitable candidate for solar cell application among all these prepared samples.

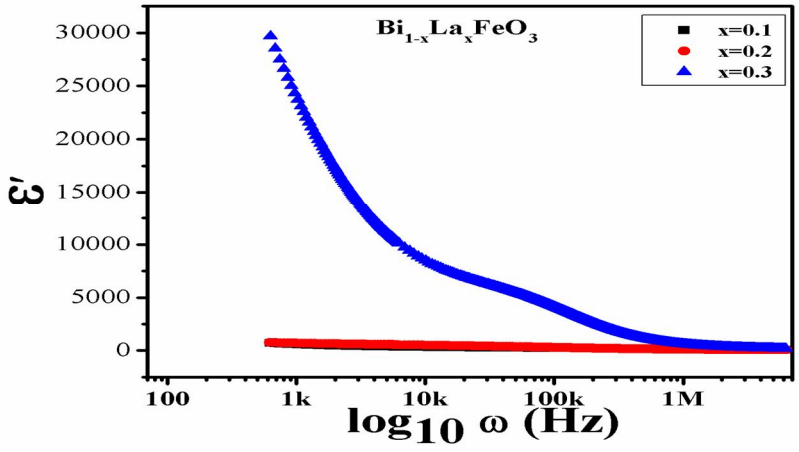

Fig. 5 (a): The frequency dependence of Dielectric constant for $Bi_{1-x}La_xFeO_3$ for x=0.1, 0.2, 0.3

ISSN: 2321-9653; IC Value: 45.98; SJ Impact Factor: 6.887
Volume 6 Issue XI, Nov 2018- Available at www.ijraset.com

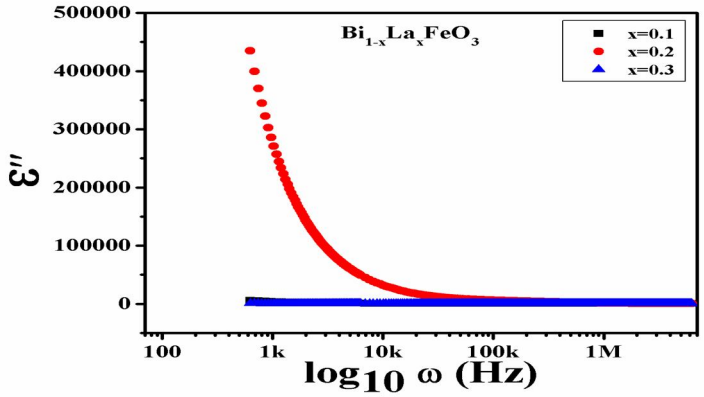

Fig. 5 (b): The frequency dependence of Dielectric loss for $Bi_{1-x}La_xFeO_3$ for x=0.1, 0.2, 0.3

The frequency dependence of electrical conductivity at room temperature for $Bi_{1-x}La_xFeO_3$ for x= 0.1, 0.2 and 0.3 is shown in figure 6. The measured dielectric data can be used to calculate the ac conductivity from the relation $\sigma_{ac} = 2\pi f \varepsilon' \varepsilon_o \tan\delta$, where parameters have their usual meaning. The results show that with increase in frequency, ac conductivity increases for all compositions. It is clear from the figure that the conductivity has two different regions within measured frequency limits, the plateau region and the dispersion region. Low frequency region corresponds to plateau region. In this region, the conductivity is independent of frequency. It gives a measure of dc conductivity. High frequency region means dispersion region. In dispersion region, the conductivity is directly proportional to the frequency. It gives a measure of ac conductivity. The frequency dependence of ac conductivity is analyzed by Jonscher's law [8] i.e $\sigma_{ac}=\sigma_{dc} + A\ \omega^n$, where "A" is the dispersion parameter and it represents the strength of polarizibility. The constant "n" is a dimensionless frequency exponent and it represents the interaction of mobile ions within same lattice [9]. Jonscher's Law states that origin of frequency dependence of conductivity lies in the relaxation phenomenon arising due to hoping of mobile charge carriers [10]. The response of mobile ions towards electric field is higher at higher frequencies due to which high conductivity is obtained at high frequencies [11].

Table 2: Various fitting parameters for conductivity vs. frequency plot

Sample	σ_{ac} (Scm^{-1})	A	n
x=0.1	4.32×10^{-5}	5.89×10^{-8}	0.66
x=0.2	3.72×10^{-1}	1.19×10^{-2}	0.18
x=0.3	1.03×10^{-4}	1.99×10^{-6}	0.42

The dc conductivity varies from 4.32×10^{-5} S/cm to 3.72×10^{-1} S/cm^1. The value of n has been found to be varying from 0.18 to 0.66. It has been noted that the value of n is less than 1 for all composition implies that the charge carriers takes a translational motion with sudden hopping [12]. Thus, the ac conductivity data reveals that sample x=0.2 exhibits higher value of electrical conductivity. The reason can be the small value of band gap of the sample.

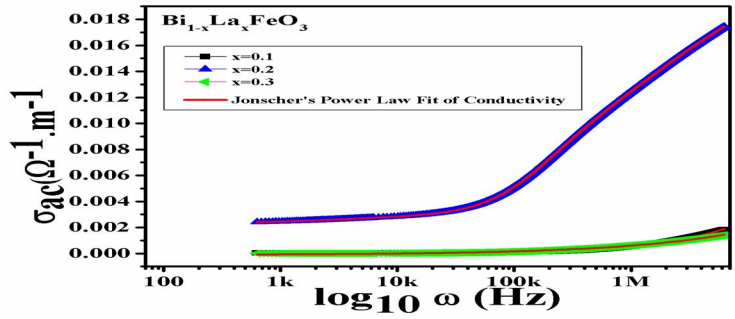

Fig. 6: Frequency dependence of electrical conductivity for $Bi_{1-x}La_xFeO_3$ (x=0.1, 0.2, 0.3)

To study the magnetic properties, Microsence E29 VSM was used. Figure 7 shows the hysteresis loop (M-H) for $Bi_{1-x}La_xFeO_3$ for concentrations varying from x=0.1 to x=0.3. It was observed under magnetic field of 15 KOe at room temperature. The graphs shows the presence of weak magnetic order for samples x=0.1, x=0.2 and x=0.3. It states that pure bismuth ferrite has anti ferromagnetic behavior below Neel Temperature with spiral spin structure [13]. But the magnetic behavior of La doped BFO is totally different from pure BFO. The graphs shows the non zero value of remnant magnetization in hysteresis loop for x= 0.1, 0.2 and 0.3. It is because of La substitution in BFO which modifies the spin structure. Due to the suppression of spins of Fe-O-Fe chains, which were anti-ferromagnetic earlier, now gives the non zero magnetic moment. It is reported that the La substitution creates a distortion in BFO due to which the bond angle of Fe-O-Fe has been changed. This type of distortion results in net magnetization of the sample [14-16]. The table indicates the increase in the value of remnant magnetization (M_r) and coercive field (H_c) with La doping from x=0.1 to 0.3, which shows the enhancement in magnetic behavior.

Table 3: Values of M_r and H_c for $Bi_{1-x}La_xFeO_3$ samples

Sample	M_r(emu/g)	H_c(KOe)
x=0.1	0.0065	1027.01
x=0.2	0.0110	1247.12
x=0.3	0.0240	2073.66

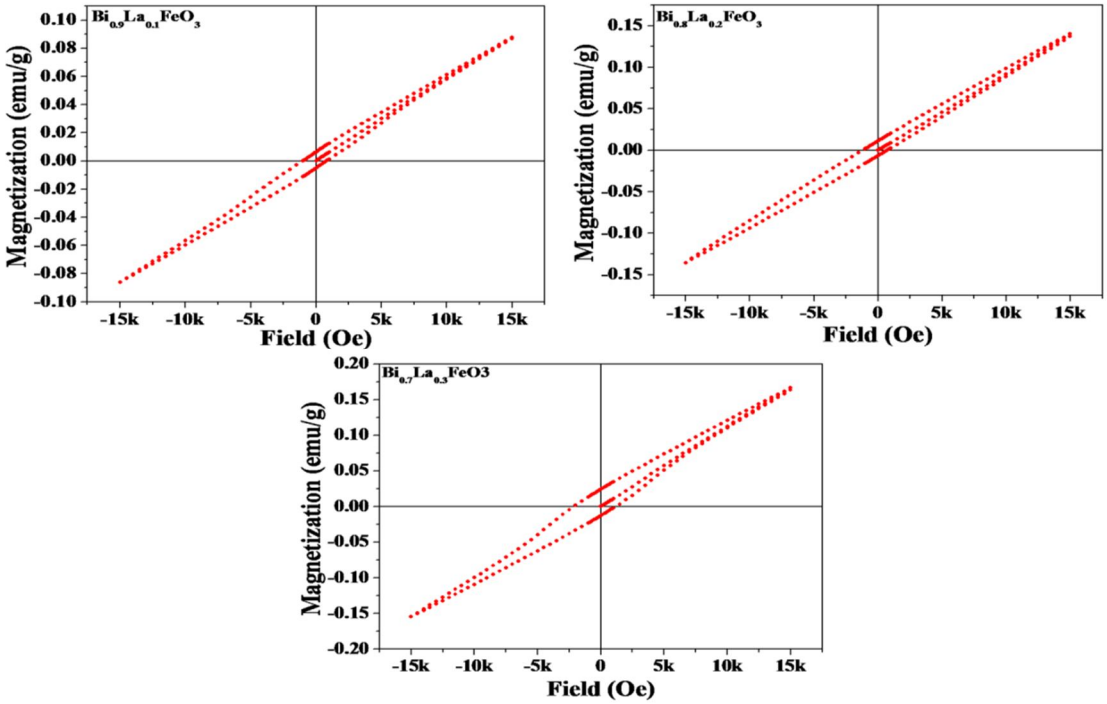

Fig. 7: The magnetization versus magnetic field (M-H) hysteresis loop for $Bi_{1-x}La_xFeO_3$ (x=0.1, x=0.2 and x=0.3)

IV. CONCLUSION

Successful synthesis of Solid solutions of $Bi_{1-x}La_xFeO_3$ ($0.1 \leq x \leq 0.3$) ceramics has been done (without any impurity phase) using solid-state-reaction method. The XRD analysis reveals that all the samples possess rhombohedral structure. The SEM micrographs clear that the grain size starts increasing from x = 0.1 to 0.2 and then decreasing from x= 0.2 to 0.3. The UV Visible spectrum reveals that the sample x=0.2 exhibit low value of band gap among all samples. La substitution in pure BFO enhances the remnant magnetization of BFO and also it has been noted that the remnant magnetization increases from x= 0.1 to 0.3. The sample x=0.2 exhibits a low value of ε' and a high value of ε'' in low frequency region implying the presence of high electric current in the sample. The ac conductivity data reveals that sample x=0.2 exhibits higher value of electrical conductivity. So, La doped Bismuth Ferrite at x=0.2 is suitable for solar cell application.

REFERENCES

[1] A. M. Bagher, M. M. Abadi Vahid, M. Mohsen, "Types of Solar Cells and Application. American Journal of Optics and Photonics." Vol. 3, No. 5, pp. 94-113, 2015.
[2] D. H. Wang, W. C. Goh, M. Ning, C. K. Ong, Appl Phy Lett., 88, 212907, 2006.
[3] G. Catalan, J. F. Scott, Adv. Mater. 21, 2463, 2009.
[4] I. Gur, N. A. Fromer, M. L. Geier, and A. P. Alivisatos, Science 310, 462, 2005.
[5] B. O'Regan and M. Grätzel, Nature London, 353, 737, 1991.
[6] K. S. Cole, H. Robert," Journal of Chemical Physics, 9, 341–351, 1941.
[7] V. Prakash, S. N. Choudhary and T. P. Sinha, "Dielectric relaxation in complex perovskite oxide BaCo1/2W1/2O3," Physica B, Vol.403, pp.103–108, 2008.
[8] D. K. Pradhan, B. Behera, P. R. Das, J. Mater. Sci. Mater. Electron, 23, 779, 2012.
[9] J. C. Dyre, Th.B. Schroder, "Ac hopping conduction at extreme disorder takes place on the percolating cluster," Phys. Stat. Sol. B, Vol. 230, pp. 5, 2002.
[10] H. Naceur, A. Megriche, M. E. Maaoui, Orient. J. Chem., Vol. 29(3), 937-944, 2013.
[11] S. Pattanayak, R. N. P. Choudhary, P. R. Das, J. Mater. Sci. Mater. Electron, 24, 2667-2771, 2013.
[12] C. Michel, J. M. Moreau, G. D. Achenbach, R. Gerson, W. J. James, Solid State Commun., 7, 701, 1969.
[13] H. L. Deng, M. Zhang, Z. Hu, Q. F. Xie, Q. Zhong, J. Z. Wei, H. Yan, J. Alloys Comp., 582, 273–276, 2014.
[14] V. A. Khomchenko, D. A. Kiselev, J. M. Vieira, L. Jian, A. L. Kholkin, A. M. L. Lopes, Y. G. Pogorelov, J. P. Araujo, M. Maglione, J. Appl. Phys., 103, 024105, 2008.
[15] A. Ianculescua, F. P. Gheorghiub, P. Postolacheb, O. Opreaa, L. Mitoseriub, J. Alloys Comp., 504, pp. 420–426, 2010.
[16] F. P. Gheorghiua, A. Ianculescub, P. Postolachea, N. Lupuc, M. Dobromira, D. Lucaa, L. Mitoseriua, J. Alloys Comp., 506, 862–867, 2010.

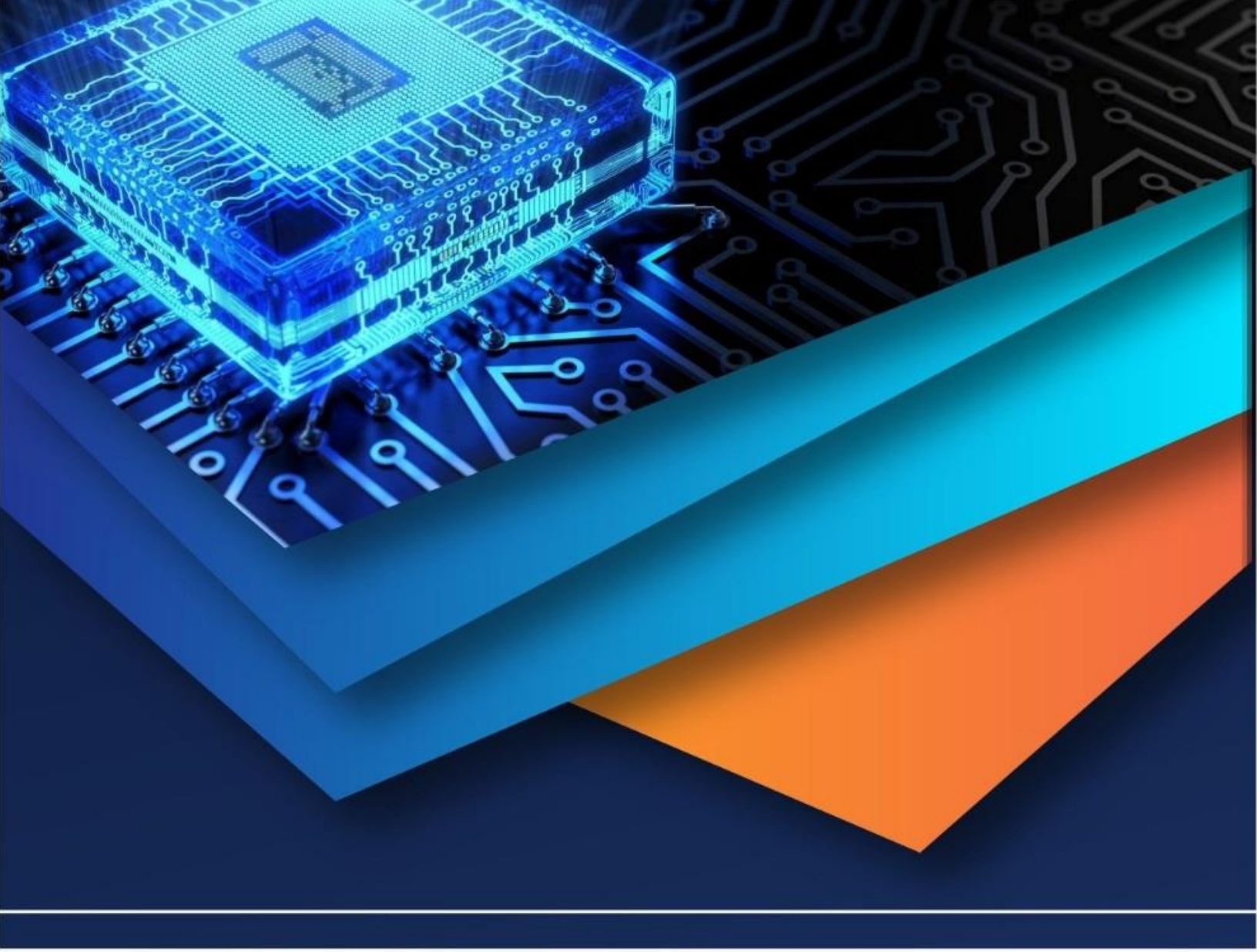

10.22214/IJRASET

45.98

IMPACT FACTOR: 7.129

IMPACT FACTOR: 7.429

INTERNATIONAL JOURNAL FOR RESEARCH

IN APPLIED SCIENCE & ENGINEERING TECHNOLOGY